Nigerian Journal of Science and Environment 2025 Volume 23 (1) 172 – 185 ISSN: 3043 – 4440
https://doi.org/10.61448/njse2312514

UTILIZATION OF ACID TREATED COCOYAM LEAF FOR CONGO RED DYE ADSORPTION: KINETICS, EQUILIBRIUM AND THERMODYNAMIC STUDIES

Ogundiran, A.A
Department of Chemical Sciences, Tai Solarin University of Education, Ijagun, Ogun State
Correspondence author's email: ogundiranaa@tasued.edu.ng (+2347066709187)

ABSTRACT

With the ever-increasing leaves of industry-induced water contamination, the focus has been shifting towards the development of environmentally friendly systems for the removal of pollutants from effluents. In the current study, batch experiments were carried out to study the adsorption capacity of acid-treated cocoyam leaf to remove Congo red dye from aqueous solution. The acid-treated adsorbent was characterized by FTIR to determine the functional groups that may be responsible for the uptake of the dye. Different experimental parameters such as the contact time, dosage, initial concentration, pH and temperature were tested. Results from the study confirmed that optimum adsorption conditions were found at a pH 2, a temperature of 40 °C at the dosage of 0.6 g and contact time of 50 min at 30 ppm. Kinetic studies showed that the adsorption of Congo red followed the Lagergren pseudo-first-order kinetic model, while the Langmuir isotherm best described the equilibrium studies. The data from the thermodynamics study disclosed that the reaction is both feasible and spontaneous. The results obtained showed that acid-treated cocoyam leaf posed a very good potential green material for Congo red dye removal.

Keywords: cocoyam leaf, Congo red, pH, Adsorption

INTRODUCTION

Environmental pollution is on the increase due to anthropogenic activities as a result of urbanization. The high increase of industrialization has its detrimental consequence on the environment, the land and the quality of water which may be available for industrial, agricultural and domestic use. There are a number of industries that make use of dyes to impart color on their finished products. Other dye industries use hazardous chemicals, which may sometimes leak into the environment as industrial waste (Aksu, 2005). The release of industrial sewages containing harmful contaminants, such as phenolics, toxic metals, and dyes, even at low concentrations, harms the environment (Khattri and Singh,2000). Dyes are the most significant pollutant due to it toxicity, persistence, non-biodegradability and potential carcinogenic properties (Garba *et al.*, 2016; Garba *et al.*, 2021). Most industries require dyes for their product, such as the textile, carpet, food, pulp, leather, printing, plastics, cosmetics, and paper sectors. The coloured wastewater from these industries, when discharged, contaminates the water bodies (Ergene *et al.,* 2009), reduces the amount of sunlight that penetrates the water bodies and also averts the process of photosynthesis, thereby reducing the activities of the aquatic plants and animals (Banat *et al.,* 2007).

Thus, effluents rich in dyes should be treated for the sake of the environment and should not be released without treatment (Lorenc-Grabowska and Gryglewicz, 2007; Abualnaja *et al.,* 2021; Alprol *et al.,* 2022; Mansour *et al.,* 2022d). At the moment, numerous physical and chemical methods like membrane filtration, electrode apparatus, chemical precipitation, chemical flocculation, electrodialysis, oxidation, reduction, crystallization, electrochemical treating, evaporator, CO2 removal, ion pair extraction, adsorption, osmosis, ion exchange, and others have been created to eliminate these pollutants from wastewater (Sharma *et al.,* 2014; Abate *et al.,* 2020; Alsas *et al.,* 2022). These methods of effluent treatment are appealing due to their efficiency, but they have several shortcomings, such as expensive operational costs, highly sophisticated and residual byproducts generated after treatment (Al-Garni *et al.,* 2013; Castellar Ortega *et al.,* 2020; Alsas *et al.,* 2022). These shortcomings prompted the effort to look for lower-cost, more environmentally friendly and more effective ways of treating industrial sewage. The process of adsorption is regarded as a viable option for eliminating synthetic contaminants from aqueous effluents (Castellar Ortega *et al.,* 2022). Adsorption is gaining attention as a method of sequestrating contaminants because of its efficacy, low energy consumption, operation ease and cost-effectiveness (Akpomie *et al.*, 2015).

Thus, this study aimed to determine whether the acid-activated cocoyam leaves can adsorb Congo red dye from aqueous solutions in batch systems.

MATERIALS AND METHODS

Collection and Preparation of Adsorbent

Cocoyam leaves were obtained on a piece of land at Lagos garage, Ijebu Ode. To remove dirt and dust from the leaves, they were washed by rubbing the leaves to ensure proper cleaning; after washing, the leaves were air-dried to prevent degradation of their active components. Following drying, a grinder was used to grind the leaves into a finely ground form, the grinding process increased the surface area of the leaf to enable improved leaf performance.

Preparation of Acidified Adsorbent

About 0.5 M of HCl was prepared, and the cocoyam leaves were placed in a large beaker and prepared. HCl solution was carefully added to the pulverised leaf powder, the mixture was stirred to ensure uniform contact of the leaf with the acid solution. The mixture was left to stand for 24 hours to modify the sample. After the desired reaction time, the mixture was decanted to separate the acid-treated leaves from the mixture, after which the leaves were rinsed off with distilled water to remove residual acid. After washing, the adsorbent was dried and placed into a well-sealed container to protect it from picking up moisture.

Preparation of Adsorbate

This solution of Congo red was made by dissolving in a beaker 0.25 g of Congo red with 500g of distilled water. The solution was mixed gently until the Congo red fully dissolved. The maximum wavelength is 498 nm.

Characterization of Adsorbent

Functional groups of the adsorbent determination were obtained using the Fourier transform infrared spectroscopy (FTIR) model 84005 (Shimadzu, Japan)

Adsorption Experiments

A batch experiment was used to conduct adsorption studies of Congo red onto acid-treated cocoyam leaf by adding 20 mL of the dye solutions at varying adsorbent doses, pH values, reaction times, and dye concentration as exemplified in Table 1 below at a temperature 25°C with a stirring rate of 200 rpm. Then, for 10 minutes and at 3000 rpm, the mixture was centrifuged. After that, a UV-visible spectrophotometer measured the highest absorbance of the solution to derive the equilibrium concentration.

The amount adsorbed at equilibrium, q_e (mg/g), was calculated by:

$$q_e = (C_i - C_e)\frac{V}{W} \qquad \text{(i)}$$

where

Ci - initial (equilibrium) dye concentration (mg/L).

Ce - final (equilibrium) concentration of dye (mg/L)

V - volume of the dye solution (L)

W - weight of the adsorbent used (g).

The dye percentage removal was calculated as follows:

$$\%\ \text{Dye removal} = \frac{Ci - Ce}{Ci} \times 100 \qquad \text{(ii)}$$

Table 1: Parameters varied during the adsorption CR

paramet Parameter	**Value range**
Dosage	0.1 g – 1 g
pH	2 - 8
time	10 – 60 min
initial concentration	5ppm-30ppm
temperature	25℃ -50 ℃

Adsorption Kinetics

Different models, including the pseudo-first-order and pseudo-second-order models, were applied to examine the kinetics of the adsorption of Congo red dye and its interaction with the adsorbents' surface during the adsorption studies focused on the duration of the process.

pseudo-first-order

The pseudo-first-order kinetics was suggested by Lagergren and Sven (1898) for the adsorption of solid/liquid systems and its formula is given as (Ho and McKay 1998)

$$\log(q_e - q_t) = \log q_e - \left(\frac{K1t}{2.303}\right) \qquad \text{(iii)}$$

q_e (mg/g) and q_t (mg/g) are the amount of dye adsorbed at a time and equilibrium, respectively, while pseudo first-order adsorption rate constants are K_1 (1/min). Experimental data were plotted as log (q_e - q_t) versus time (t) and K_1 was used to treat.

Nigerian Journal of Science and Environment 2025 Volume 23 (1) 172 – 185 ISSN: 3043 – 4440
https://doi.org/10.61448/njse2312514

The slope and intercept of the plot were used to determine the values of $K_1$and q_e

pseudo-second-order

The linear form of the pseudo-second-order kinetic model can be expressed as (Ho and McKay 1998)

$$\frac{t}{q_t} = \frac{1}{k_2 q_e^2} + \frac{t}{q_e} \quad \text{(iv)}$$

where

The rate constant of pseudo-second-order adsorption, k2 (g/(mg min)), is found from the linear plots of t/qt with time t. The slope and intercept of the plot and the values qe of and k2 were calculated from the values of the plot. (Edokpayi et al., 2015).

Adsorption Isotherms

Equilibrium data obtained from the adsorption study at different concentrations and temperatures were analyzed using Langmuir and Freundlich adsorption isotherm models to determine adsorption behavior of solutes on the surface of the adsorbent.

Langmuir Isotherm

According to the Langmuir model, adsorbates will be sorbed onto the surface of an ideal adsorbent at a fixed number of predetermined positions, and every position can only hold an individual molecule (Mwangi et al., 2012). Adsorption of adsorbate is assumed to occur without interaction with already adsorbed ionic species (Edokpayi *et al.,* 2015). The linearized expression for the Langmuir model is represented by (Langmuir, 1916);

$$\frac{1}{\mathrm{qe}} = \frac{1}{q_{max}} + \left(\frac{1}{K_L q_{max}}\right)\frac{1}{C_e} \quad \text{(v)}$$

q_e and q_{max} are the amounts (mg/g) of dye adsorbed per unit mass of adsorbent and maximum adsorption capacity at equilibrium, respectively, Ce is the equilibrium concentration of adsorbate, while K_L (Lmg-1) is the Langmuir constant.

Freundlich Isotherm

The quantitative relationship relating the proportion of the ionic compound absorbed by the adsorbent to the concentration of the ionic compound dissolved in the solvent. This is more relevant to adsorption processes involving heterogeneous surfaces and may be written linearly. (Freundlich, 1907)

$$log q_e = log K_F + \frac{1}{n} log C_e \quad \text{(vi)}$$

where

The quantity of dye adsorbed at equilibrium (mg g-1), and a rough valuation of the adsorption capacity of the adsorbent, KF (mg g-1), is q_e. 1/n is adsorption intensity adsorption indicating heterogeneity of adsorbent site and the energy of distribution (Olorundare *et al.,* 2014).

Adsorption Thermodynamics

The thermodynamic parameters, ΔG^o, ΔH^o and ΔS^o indicate the adsorbate and adsorbent energy-friendly interactions, the feasibility, and the spontaneity of the reaction during the adsorption process (Adeogun *et al.,* 2016). These parameters were calculated using the following equations.

$$\Delta G^\circ = -RT\ln K_D \quad \text{(vii)}$$

$$\Delta G^\circ = \Delta H^\circ - T\Delta S^\circ \quad \text{(viii)}$$

$$\ln K_D = \frac{\Delta S^\circ}{R} - \frac{\Delta H^\circ}{RT} \quad \text{(ix)}$$

where

The Van't Hoff plot, the slope and intercept of the adsorption process, is given by ($\ln K_D$ vs 1/T)
where thermodynamic parameters were obtained from. The universal gas constant (R = 8.314 J/mol/K), temperature (T absolute and equilibrium constant (K_D) is the distribution coefficient (qe/Ce). (Singh *et al.,* 2020)

RESULTS AND DISCUSSION

FTIR Characterization

The FTIR spectrum of acidified cocoyam leaf used for dye adsorption is displayed in Figure 1. The FTIR spectrum enabled the discovery of the functional groups on the adsorbent surface. The peak observed at around 3475cm-1 denotes the presence of OH stretching carboxylic acid and phenol (Prahas, 2008), while the band at around 2932cm^{-1}-2850cm-^{1} represents C-H stretching of sp^3 hybridization (Viana *et al.,* 2012). The absorption bands at 1680 and 1640 cm-1 represent C=C, stretching of the unsaturated carboxylic group and C=O of amide group. The peak at 1140.63 cm^{-1} corresponds to the C-O bond of the aliphatic ester group (El Hendawy, 2006). The bands between 1325 to 1429 cm^{-1} represent the C-O bond of phenols (Vaghetti *et al.,* 2009).

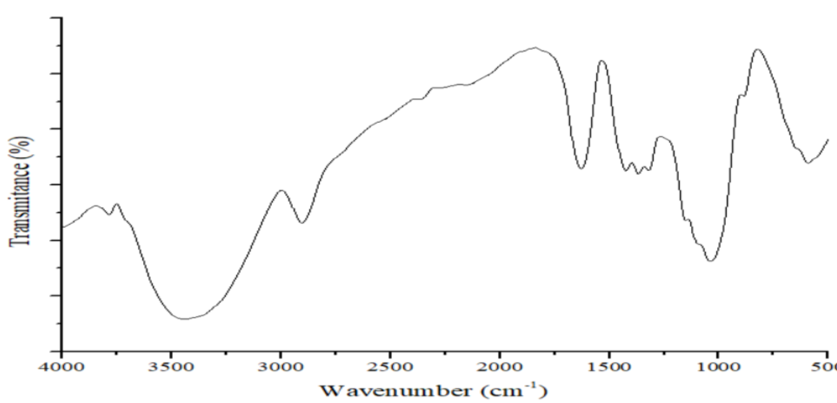

Figure 1: FTIR Spectrum of Acidified cocoyam leaf sample

Effect of Time and Concentration

Figure 2 presents the impact of initial dye concentration versus contact time. Contact time and dye concentration influenced the amount of dye removed. The amount of dye absorbed at equilibrium from increased 0 mg/g dyed in water (5 ppm) reached the maximum value of 11.22 mg/g dyed at 30 ppm. After equilibrium was achieved, Congo red dye removal did not increase significantly. This has the effect of increasing the interaction between Congo red and the adsorbent as more adsorption sites are reached, thus increasing the adsorption capacity (Yagub *et al.,* 2014)

The plot clearly shows that the initial dye adsorption was high; however, in later stages, the rate of adsorption became constant, which reflected that the available site for the adsorption was near saturation after 50 min (Hu *et al.,* 2010). The results indicated that the maximum amount of dye adsorbed at

Nigerian Journal of Science and Environment 2025 Volume 23 (1) 172 – 185 ISSN: 3043 – 4440
https://doi.org/10.61448/njse2312514

equilibrium in the adsorption process is 11.22 mg/g at 30 ppm concentration after 50 min of contact time. Adsorption efficiency reduced after it reached the equilibrium and was attributed to the saturation of the adsorbent surface with Congo red molecules (Taher *et al.,* 2017: Ogundiran *et al.,* 2022)

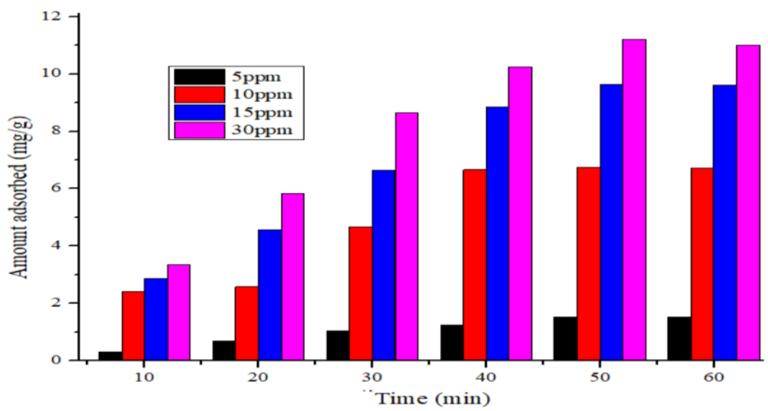

Figure 2: Time and Concentration plot for adsorption of Congo red by acidified cocoyam leaf.

Effect of Solution pH

The effect of pH is presented graphically in Figure 3. The pH of a solution is significant in the study of adsorption because of its impact on the available site on the adsorbent and how it interacts with dye molecules (Lafi *et al.,* 2019; Jain and Sikarwar, 2014). The plots of the experimental results, as presented in Figure 3, indicate that the optimal pH was 2, at which the percentage of dye molecules removed was the highest (76.45%). When the pH was increased from 3 to 8, the efficiency of the dye removal reduced. The maximum adsorption of Congo red at pH 2 is due to the strong electrostatic force that exists between the dye molecule and the surface charge of the adsorbent. (Lafi *et al.,* 2019).

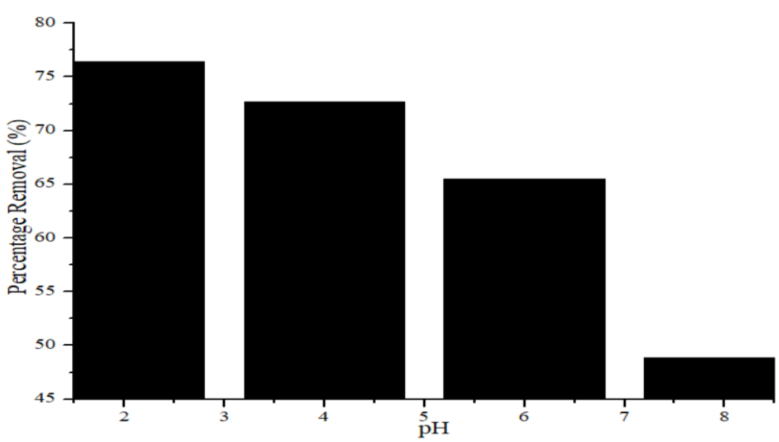

Figure 3: Effect of pH on adsorption of Congo red by acid-treated cocoyam leaf.

Effect of Temperature

Figure 4 presents the relationship between Congo red dye adsorption at varying temperatures from aqueous solution by cocoyam leaf using the acidified solution. As seen in the plots, the Congo red removal was higher as temperatures increased; thus, an endothermic adsorption phenomenon can be suggested. The percentage removal of Congo red was increased from 50.00 % to 69.34 %, with an increase in temperature from 25 to 40 °C. When the temperature continued to rise beyond 40 °C, there was no noticeable removal of Congo red. The research done by Olakunle *et al.,* (2018), using activated cocoa pod husk for the adsorption of Congo red, showed similar results with higher temperatures.

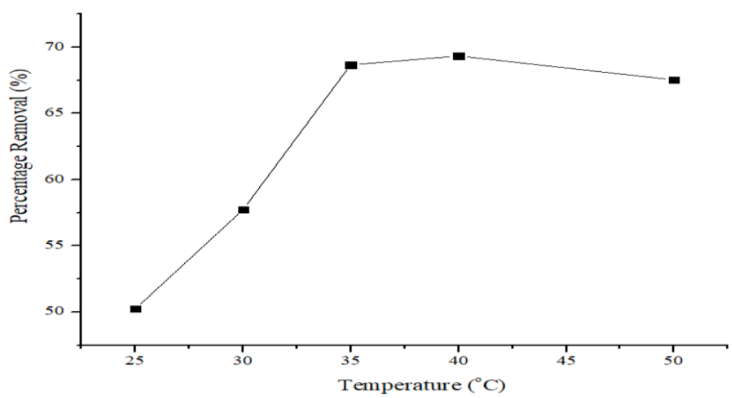

Figure 4: Plots of temperature effect for the adsorption of Congo red by acid-treated cocoyam leaf.

Effect of Biomass Dosage

Figure 5 shows the removal efficiency of Congo red to the amount of adsorbent used. Figure 5 also shows that the removal percentage increased from 48.82% to 75.41% when the adsorbent was increased from 0.1g to 0.6 g, after which there was no further improvement in the removal percentage as the adsorbent dosage increased. In the case of Congo red adsorption with cocoyam leaf, the percentage removal of Congo red with an increase in adsorbent dosage was due to the increased number of vacant sites available for adsorption on the cocoyam leaf surface (Vaghetti *et al.,* 2009). The change in the concentration of dye removal percentage in compliance with the concentration of biosorbent is consistent with reports on the adsorption of dye (Wanyonyi *et al.,* 2014; Asses *et al*., 2018; Ogundiran *et al.,* 2022).

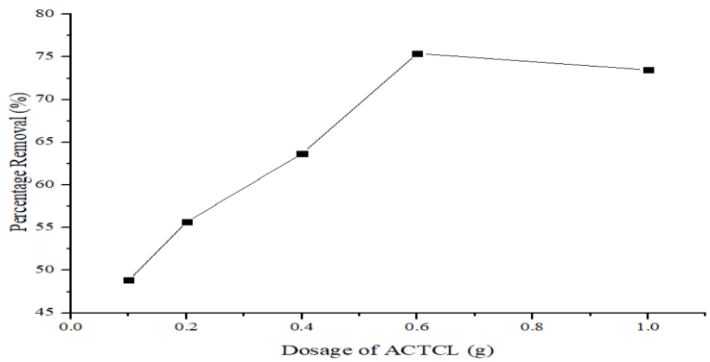

Figure 5: Varying dosage plot of the adsorption of Congo red by acid-treated cocoyam leaf.

Adsorption Kinetics

Figures 6 and 7 show the graphical representation of kinetic models, while the parameters that were calculated are displayed in Table 2. From the results obtained, the adsorption of Congo red dye onto the adsorbent best-fit model is pseudo-first-order based on its correlation coefficients (R^2) values of (0.98-0.99) at different concentrations of the dye, which are greater than those of the pseudo-second-order model. In addition, the $q\,e$ experimental and $q\,e$ calculated values of the pseudo-first-order were in agreement compared to those of the pseudo-second-order. The lower %SSE values for the pseudo first-order model also showed that the Congo red adsorption was favoured by pseudo first order. This also showed that the kinetic data of the adsorption system was well described by pseudo first order kinetics

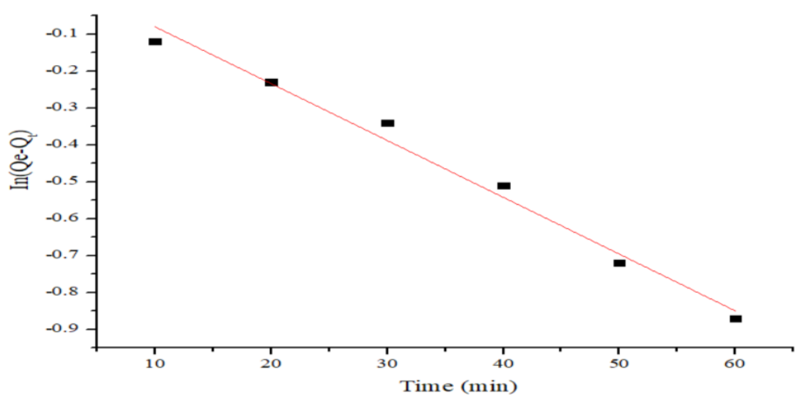

Figure 6: Pseudo-first-order model

Nigerian Journal of Science and Environment 2025 Volume 23 (1) 172 – 185 ISSN: 3043 – 4440
https://doi.org/10.61448/njse2312514

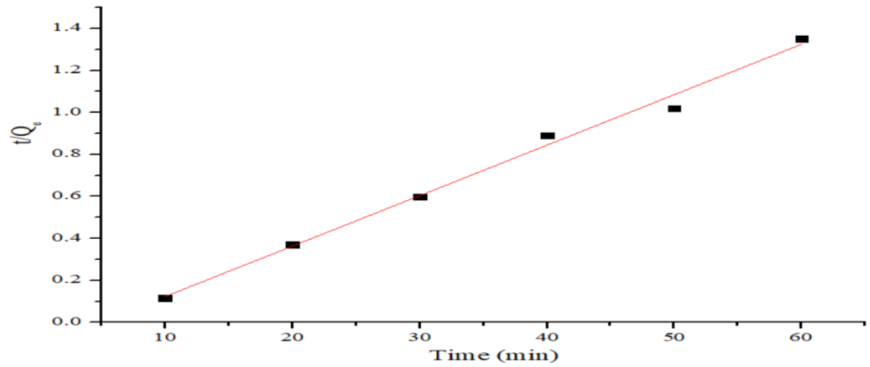

Figure 7: Pseudo-second-order model

Table 2: Kinetic Model Parameter for Congo red removal

	Pseudo-First order						pseudo- Second order			
Co	C_e	q_e(exp)	q_e(cal)	K_1	R^2	%SSE	q_e(cal)	K_2	R^2	%SSE
5	3.5	1.53	1.32	0.032	0.996	0.041	2.44	0.016	0.945	0.179
10	5.65	6.760	5.98	0.044	0.997	0.035	4.44	0.0175	0.967	0.103
15	8.15	9.630	10.22	0.14	0.989	0.018	7.88	0.0139	0.978	0.055
20	10.22	11.220	11.45	0.33	0.997	0.006	9.22	0.1102	0.958	0.054
25	12.33	13.220	13.1	0.52	0.989	0.003	10.25	0.124	0.968	0.068

Adsorption Isotherms

Isothermal studies are mainly used to determine the conditions for which high adsorption capacities will be obtained and then evaluate the shape of the isotherm plots (Sohn and Kim, 2005). The isotherm parameters for CR adsorption onto acid treated cocoyam leaf are shown in Figures 8 and 9 while in Table 3, isotherm models' parameters are presented. The results indicated that while both the model equations suit the experimental equilibrium data for adsorption isotherms for Congo red, the Langmuir isotherm model provides a more reasonable fit than the Freundlich model. This is shown by examining the coefficients of determination for two models, Langmuir model has the highest R^2 values of (0.989). It could also be observed from Table 3 that the R_L value was 0.25 which indicates a favourable adsorption process. It was also observed from the Freundlich constants that the R^2 value (0.96) was lower than that of Langmuir model, thus signifying poor fitting while the value of 1/n (0.360) fell below 1 signifying a normal and favourable adsorption process for the uptake of Congo red.

Nigerian Journal of Science and Environment 2025 Volume 23 (1) 172 – 185 ISSN: 3043 – 4440
https://doi.org/10.61448/njse2312514

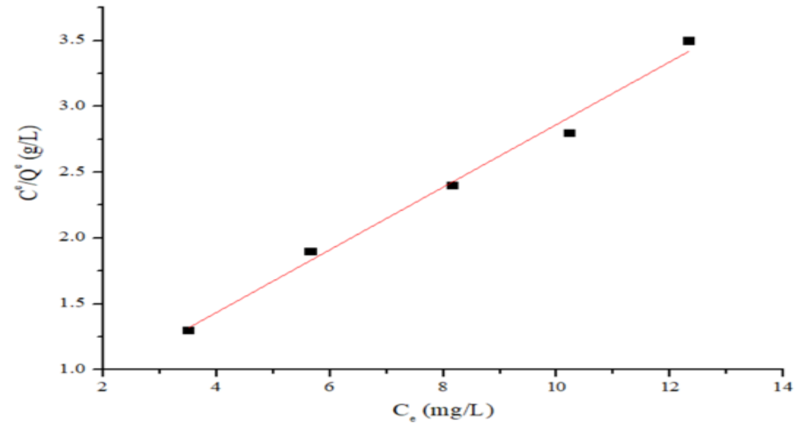

Figure 8: Langmuir Model Isotherm

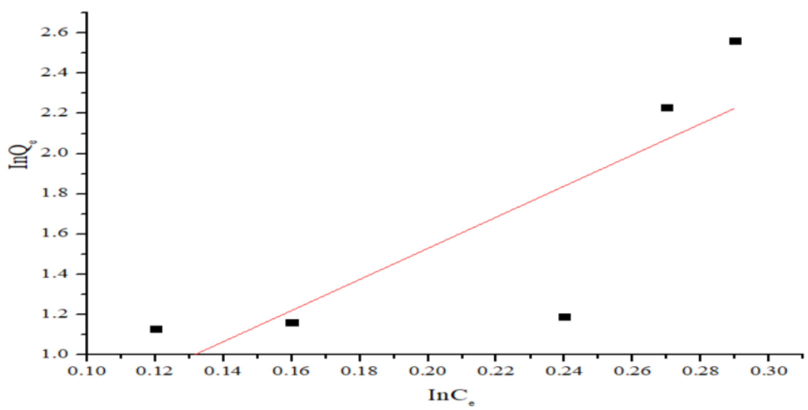

Figure 9: Freundlich model isotherm

Table 3: Isotherm Model Parameters for Adsorption of Congo Red Dye

Isotherms			
Langmuir		Freudlich	
Q_{max}	10.45	Kf	8.36
R_L	0.25	1/n	0.360
R^2	0.989	R^2	0.966

Adsorption Thermodynamics

Table 4 displays the values acquired for the parameters, while Figure 10 displays the linear graph for the adsorbent derived from the Vant Hoff plot of In K_D against (1/T). As for adsorbing Congo red from the aqueous on the acidified cocoyam leaf, all working temperatures produced negative ΔG° values. This suggests that the adsorption process was spontaneous and feasible. The positive ΔH° value supported this with the fact that the process of adsorption is endothermic. The positive ΔS° suggests a greater disorder at the interface of the adsorbent and the adsorbate, owing to the active sites on the adsorbent where the molecules of Congo red dye are attached. This has also been observed by other researchers in the case of adsorption of Congo red onto acid-modified crab shell powder (Rao and Rao, 2016) and acid-modified walnut shell powder (Ojo *et al.,* 2019).

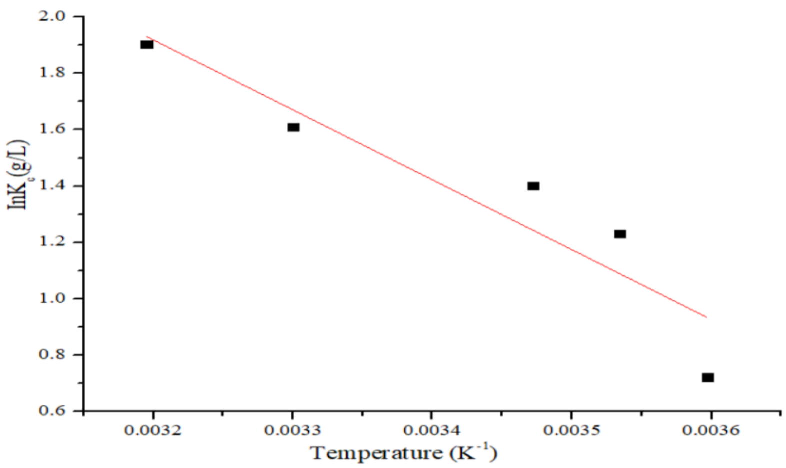

Figure 10: Van't Hoff plots of Congo red adsorption onto acid-treated cocoyam leaf.

TABLE 4: Thermodynamic Parameters for Congo Red Dye Adsorption onto Acid Treated Cocoyam Leaf.

InK	1/T+273	T°C	ΔG°	ΔH°	ΔS°
0.722	0.003597	25	-1.32		
1.231	0.003534	30	-1.81		
1.401	0.003472	35	-2.45	+20.82	+2.44
1.610	0.0033	40	-2.87		
1.904	0.003195	50	-2.92		

Conclusion

The current research investigates the impact of different adsorption conditions on adsorption efficiency alongside kinetic, equilibrium, and thermodynamic studies. Increasing the dosage of adsorbent and contact time led to a percentage increase in dye uptake, while the removal of Congo red increased at a higher initial dye concentration. The uptake percentages of Congo red decreased with a pH increase and temperatures above 40°C. The kinetic adsorption study was best described with pseudo first-order kinetics, while the equilibrium adsorption of dye was best described by the Langmuir isotherm, which had a better correlation coefficient R2 than the Freundlich isotherm. The results of the thermodynamic study support that the adsorption of Congo Red dye on activated cocoyam leaf was feasible, spontaneous, and endothermic. This study supports the hypothesis that activated cocoyam leaf can effectively remove some pollutants from the aqueous phase.

REFERENCES

Abate, G. Y., Alene, A. N., Habte, A. T., & Getahun, D. M. (2020). Adsorptive removal of malachite green dye from aqueous solution onto activated carbon of Catha edulis stem as a low cost bio-adsorbent. *Environmental Systems Research*, *9*, 1-13.

Abualnaja, K. M., Alprol, A. E., Ashour, M., & Mansour, A. T. (2021). Influencing multi-walled carbon nanotubes for the removal of ismate violet 2R dye from wastewater: isotherm, kinetics, and thermodynamic studies. *Applied Sciences*, *11*(11), 4786.

Adeogun, A. I., Idowu, M. A., Akiode, K. O., & Ahmed, S. A. (2016). Bioremediation of Cu (II) contaminated water by Saccharum officinarum: effect of oxalic acid modification on equilibrium, kinetic and thermodynamic parameters. *Bioresources and Bioprocessing*, *3*, 1-16.

Akpomie, K. G., Dawodu, F. A., & Adebowale, K. O. (2015). Mechanism on the sorption of heavy metals from binary-solution by a low cost montmorillonite and its desorption potential. *Alexandria Engineering Journal*, *54*(3), 757-767.

Aksu, Z. (2005). Application of biosorption for the removal of organic pollutants: a review. *Process biochemistry*, *40*(3-4), 997-1026.

Al-Garni, S. M., Ghanem, K. M., Kabli, S. A., & Biag, A. K. (2013). Decolorization of Crystal Violet by Mono and Mixed Bacterial Culture Techniques Using Optimized Culture Conditions. *Polish Journal of Environmental Studies*, *22*(5).

Alprol, A. E., Heneash, A. M., Ashour, M., El-Kafrawy, S., & Soliman, A. M. (2022). Chemical assessment of water quality, heavy metals, and the distribution of zooplankton communities, based on field and GIS data in the drains of Burullus Lake, Egypt. *Arabian Journal of Geosciences*, *15*(18), 1511.

ALSAS, S. A., Garba, Z. N., & Sallau, M. S. (2022). Nickel adsorption onto sweet dattock shell: statistical error function models as parametric isotherm predictors. *FUDMA JOURNAL OF SCIENCES*, *6*(2), 208-220.

Asses, N., Ayed, L., Hkiri, N., & Hamdi, M. (2018). Congo red decolorization and detoxification by Aspergillus niger: removal mechanisms and dye degradation pathway. *BioMed research international*, *2018*(1), 3049686.

Banat, F., Al-Asheh, S., Al-Ahmad, R., & Bni-Khalid, F. (2007). Bench-scale and packed bed sorption of methylene blue using treated olive pomace and charcoal. *Bioresource technology*, *98*(16), 3017-3025.

Castellar-Ortega, G. C., Cely-Bautista, M. M., Cardozo-Arrieta, B. M., Angulo-Mercado, E. R., Mendoza-Colina, E. D. J., Zambrano-Arevalo, A. M., ... & Rosales-Díaz, C. L. (2020). Removal of the direct navy-blue dye on modified coffee bean. *Tecnología y ciencias del agua*, *11*(4), 1-26.

Edokpayi, J. N., Odiyo, J. O., Msagati, T. A., & Popoola, E. O. (2015). A Novel Approach for the removal of lead (II) ion from wastewater using mucilaginous leaves of diceriocaryum eriocarpum plant. *Sustainability*, *7*(10), 14026-14041.

El-Hendawy, A. N. A. (2006). Variation in the FTIR spectra of a biomass under impregnation, carbonization and oxidation conditions. *Journal of Analytical and Applied Pyrolysis*, *75*(2), 159-166.

Ergene A, Ada K, Tan S, Katircioğlu H (2009) Removal of Remazol Brilliant Blue R dye from aqueous solutions by adsorption onto immobilized Scenedesmus quadricauda: Equilibrium and kinetic modeling studies. Desalination 249:1308-1314

Freundlich, H. (1907). Über die adsorption in lösungen. *Zeitschrift für physikalische Chemie*, *57*(1), 385-470.

Garba, A., Nasri, N. S., Basri, H., Ismail, R., Abdul Majid, Z., D. Hamza, U., & Mohammed, J. (2016). Adsorptive removal of phenol from aqueous solution on a modified palm shell-based carbon: fixed-bed adsorption studies. *Desalination and Water Treatment*, *57*(60), 29488-29499.

Garba, Z. N., Abdullahi, A. K., Haruna, A., & Gana, S. A. A. (2021). Risk assessment and the adsorptive removal of some pesticides from synthetic wastewater: a review. *Beni-Suef University Journal of Basic and Applied Sciences*, *10*, 1-18.

Ho, Y. S., & McKay, G. (1998). Sorption of dye from aqueous solution by peat. *Chemical engineering journal*, *70*(2), 115-124.

Hu, L., Hu, X., Wu, X., Du, C., Dai, Y., & Deng, J. (2010). Density functional calculation of transition metal adatom adsorption on graphene. *Physica B: Condensed Matter*, *405*(16), 3337-3341.

Jain, R., & Sikarwar, S. (2014). Adsorption and desorption studies of Congo red using low-cost adsorbent: activated de-oiled mustard. *Desalination and Water Treatment*, *52*(37-39), 7400-7411.

Khattri, S. D., & Singh, M. K. (2000). Colour removal from synthetic dye wastewater using a bioadsorbent. *Water, Air, and Soil Pollution*, *120*, 283-294.

Lafi, R., Mabrouk, W., & Hafiane, A. (2019). Removal of Methylene blue from saline solutions by adsorption and electrodialysis. *Membr. Water Treat*, *10*(2), 139-148.

Lagergren, S., & Sven, K. (1898). Vetenskapsakad. *Handl*, *24*, 1-39.

Langmuir, I. (1916). The evaporation, condensation and reflection of molecules and the mechanism of adsorption. *Physical Review*, *8*(2), 149.

Lorenc-Grabowska, E., & Gryglewicz, G. (2007). Adsorption characteristics of Congo Red on coal-based mesoporous activated carbon. *Dyes and pigments*, *74*(1), 34-40.

Mansour, A. T., Alprol, A. E., Abualnaja, K. M., El-Beltagi, H. S., Ramadan, K. M., & Ashour, M. (2022). Dried brown seaweed's phytoremediation potential for methylene blue dye removal from aquatic environments. *Polymers*, *14*(7), 1375.

Mohan Rao, T., & Venkata Basava Rao, V. (2016). Biosorption of Congo Red from aqueous solution by crab shell residue: a comprehensive study. *Springerplus*, *5*, 1-14.

Ogundiran, A. A., Ofudje, E. A., Ogundiran, O. O., & Adewusi, A. M. (2022). Cationic dye adsorptions by eggshell waste: kinetics, isotherms and thermodynamics studies. *Desalin Water Treat*, *280*, 157-167.

Ojo, T. A., Ojedokun, A. T., & Bello, O. S. (2019). Functionalization of powdered walnut shell with orthophosphoric acid for Congo red dye removal. *Particulate science and technology*, *37*(1), 74-85.

Olakunle, M. O., Inyinbor, A. A., Dada, A. O., & Bello, O. S. (2018). Combating dye pollution using cocoa pod husks: a sustainable approach. *International Journal of Sustainable Engineering*, *11*(1), 4-15.

Olorundare, O. F., Msagati, T. A. M., Krause, R. W., Okonkwo, J. O., & Mamba, B. B. (2014). Steam activation, characterisation and adsorption studies of activated carbon from maize tassels. *Chemistry and Ecology*, *30*(5), 473-490.

Sharma, K., Kaith, B. S., Kumar, V., Kalia, S., Kumar, V., & Swart, H. C. (2014). Water retention and dye adsorption behavior of Gg-cl-poly (acrylic acid-aniline) based conductive hydrogels. *Geoderma*, *232*, 45-55.

Singh, S., Kumar, V., Datta, S., Dhanjal, D. S., Sharma, K., Samuel, J., & Singh, J. (2020). Current advancement and future prospect of biosorbents for bioremediation. *Science of the Total Environment*, *709*, 135895.

Taher, T., Mohadi, R., Rohendi, D., & Lesbani, A. (2017, March). Kinetic and thermodynamic adsorption studies of congo red on bentonite. In *AIP Conference Proceedings* (Vol. 1823, No. 1). AIP Publishing.

Viana, R. B., Da Silva, A. B., & Pimentel, A. S. (2012). Adsorption of sodium dodecyl sulfate on Ge substrate: the effect of a low-polarity solvent. *International journal of molecular sciences*, *13*(7), 7980-7993.

Wanyonyi, W. C., Onyari, J. M., & Shiundu, P. M. (2014). Adsorption of Congo red dye from aqueous solutions using roots of Eichhornia crassipes: kinetic and equilibrium studies. *Energy Procedia*, *50*, 862-869.

Yagub, M. T., Sen, T. K., Afroze, S., & Ang, H. M. (2014). Dye and its removal from aqueous solution by adsorption: a review. *Advances in colloid and interface science*, *209*, 172-184.